大規模な人の移動データを活用した歩行行動に対する環境特性の影響

黎 雯静 [1]・柴崎 亮介 [2]・秋本 和紀 [4]・張 浩然 [5]・小林 博樹 [6]

[1] 東京大学空間情報科学研究センター（〒277-8568 千葉県柏市柏の葉 5-1-5）
E-mail: liwenjing@csis.u-tokyo.ac.jp
[2] 麗澤大学（〒277-8686 千葉県柏市光ヶ丘 2-1-1）
E-mail: shiba@csis.u-tokyo.ac.jp
[4] Geo Technologies 株式会社（〒113-0021 東京都文京区本駒込 2-28-8）
E-mail: k_akimoto@geot.jp
[5] LocationMind 株式会社（〒101-0048 東京都千代田区神田司町 2-8-1）
E-mail: h.zhang@pku.edu.cn
[6] 東京大学情報基盤センター（〒277-0882 千葉県柏市柏の葉 6-2-3）
E-mail: kobayashi@ds.itc.u-tokyo.ac.jp

歩行者の歩行経路選択において、沿道環境がこれらの選択に与える影響を理解することは、歩行者に優しい都市を設計する上で重要である。過去の研究では、建築環境による影響の分析は歩行行動（歩行者の総流れなど）とマクロレベルの環境特性に限定されていた。本研究は、人々の移動に関する大規模な GPS データを用いて、微細レベルな環境特性が個々の歩行者の迂回行動に与える影響を調査することを目的とする。まず、GPS 歩行軌跡から検出された歩行者の実際の選択経路と利用可能な最短経路とを比較し、東京の各通りに対して歩行者の選好を表す迂回スコアを新たに提案した。次に、土地利用、交通条件、自然の特徴、商業施設などの様々な建築環境特性を測定した。微視的な通りの特徴を抽出するために、Google ストリートビューの画像をコンピュータビジョン技術を用いて解析した。そして歩行経路選択と相関する環境特性を特定した。この研究は、マイクロスコピックな環境要因が歩行経路選択に与える影響を数量化する試みであり、持続可能なライフスタイルを推進するためのガイドラインと介入策を設計する際に有益な示唆を提供する。

Key Words: *ビッグモビリティデータ, 歩行者選択, 建築環境, コンピュータビジョン*

1. INTRODUCTION

Walking, as a fundamental mode of transportation, plays an indispensable role in urban sustainability, quality of life, resident health, economy, and social interaction. The built environment, which refers to the physical surroundings where people live, work, and recreate, significantly impacts pedestrian behaiors [1], [2]. Understanding the influence of the built evironment on pedestrian pathway choices is crucial for designing pedestrian-friendly cities.

Currently, extensive research has been conducted on urban walkability. These walkability research indicators encompass numerous built environment features believed to affect pedestrian mode choice and behavior, such as transportation [3], POI [4], nature environment [5], and so on. However, in previous studies on the built environment and pedestrian behavior, there remain some knowledge gaps that have yet to be fully addressed.

Firstly, analyses of pedestrian behavior have seldom discussed the actual walking routes and their relationship with the shortest paths. Some prior studies focused on the probability of walking mode choices in comparison with other modes of transportation [6], [7]. Some research centered on the geographical locations of the walk trip's origin and destination [8],

rather than the walking experience during the journey itself. Others delved deeper to study aggregated pedestrian flows on each segment [9] or individuals' walking speeds [10]. The actual walking routes and their relationship with the shortest paths have been rarely discussed. In reality, not all pedestrians opt for the shortest routes; there are systematic deviations. These aggregated individual deviations reveal information about the built environment features that attract pedestrian movement. While a few emerging studies have examined the discrepancies between route preferences and the shortest paths [11], [12], these can serve as a valuable reference for studying walking route preferences. However, route preferences may vary between different cities. Thus, there is a need for better knowledge to study the deviation between the real walking route choices and the shortest paths in the Tokyo urban environment.

Secondly, literature regarding pedestrian walking preferences is predominantly based on small-scale individual preference estimations, field surveys, or travel questionnaire reports [13], and is typically limited to smaller geographic settings, such as neighborhood blocks. Due to data source limitation, these studies are not enough in understanding the individual level travel route preferences under fine spatiotemporal granularity and fail to offer a comprehensive large-scale view of the entire city. Recent endeavors have employed advanced data collection methodologies to elucidate the relationship between pedestrian movement and the built environment. Examples include route recommendations from Google Navigation API [14], wearable devices [15], and mobile phone GPS data [16] to construct a more comprehensive measure of walking behaviors. GPS trajectories offer a valuable data source for studying individual-level walking behaviors, demonstrating advantages in both spatiotemporal granularity and scale of research.

Thirdly, in terms of measurement methodology of the built environment, existing studies about the influence of the built environment on walking behaviors primarily focus on macro-level measurement indicators, including land use types, density, infrastructure and so on. The relationship between the more detailed, eye-level micro-scale street environments and walking preferences is less frequently examined. Utilizing Street View Image (SVI), Computer Vision (CV), and Deep Learning (DL) algorithms allow us to measure micro-scale street features efficiently at a high throughput.

To address the aforementioned research gaps, this study utilizes large-scale individual-level GPS trajectories and proposes a novel score that reflects the pedestrian detour preference for each street. By integrating SVI data with CV techniques, we measured micro-scale built environment features and quantified the influence of micro-level built environment factors on individual detour behaviors.

The Asakusa – Sumidagawa - Tokyo Skytree area serves as the case study of this paper. it is one of the Tokyo's iconic waterfront spaces and walking routes. Currently, Tokyo is allocating a larger budget to bolster active transportation infrastructure to encourage walking activities and enhance the quality of urban life. A thorough understanding of how walkers interact with street will enable urban planners and policymakers to prepare practical design guidelines, aiding in crafting a supportive walking environment to sustainably increase walking activities and further invigorate urban life. This study offers valuable insights for designing guidelines and interventions promoting sustainable lifestyles.

The rest of the paper is organized as follows: Section 2 describes the research framework and methods used in details. Section 4 presents our study case. . Section 5 gives a comprehensive analysis of the simulation results. Finally, Section 6 provides the conclusion of the research.

2. STUDY AREA

The Asakusa (浅草) – Sumidagawa (隅田川) - Tokyo Skytree area（東京スカイツリー）(**Figure 1**) serves as the case study of this paper. It is one of the Tokyo's iconic waterfront spaces and walking routes. There are eight subway stations in this area. The sightseeing spots including Tokyo Skytree, Sumida Park, Sensoji Temple, and so on.



Figure 1. Study area

3. DATASET AND METHODLOGY

3.1 Research Framework

This study aims to quantify the influence of micro-level built environment factors on individual detour behaviors. Firstly, we compared the actual pedestrian paths detected from GPS walking trajectories with

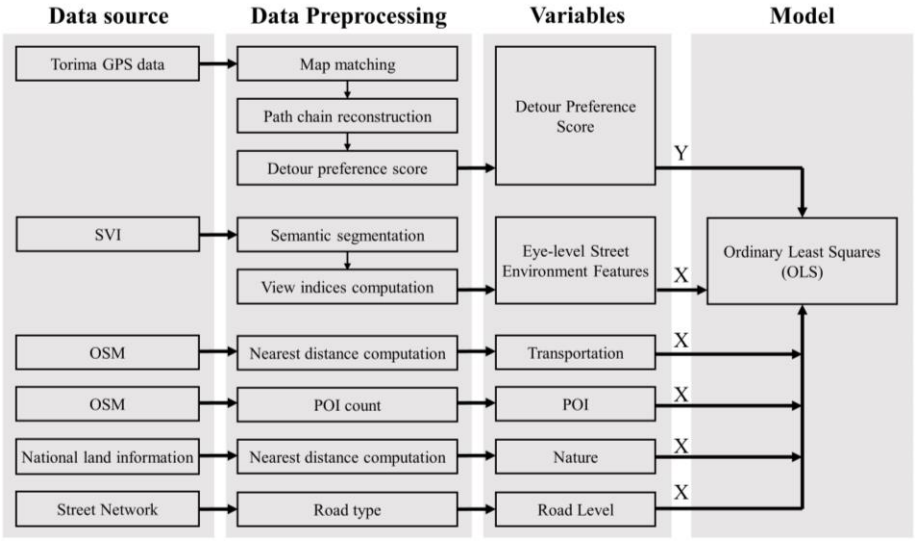


Figure 2. Research Framework

the shortest available routes, and introduced a novel score that reflects the detour preference of pedestrians for each street. Secondly, we measured various built environment features using multi-source data, including land use, traffic conditions, natural features, and commercial facilities, among others. To extract micro-scale street features, we employed CV techniques to analyze Google Street View images. Following this, through regression analysis, we identified environmental characteristics associated with walking path choices. The framework of this study is showed in **Figure 2**.

3.2 Dependent Variable: Pedestrian Detour Preference Score

This section introduces the computation method for the dependent variable - the pedestrian detour preference score. **Figure 3** shows the computation process.

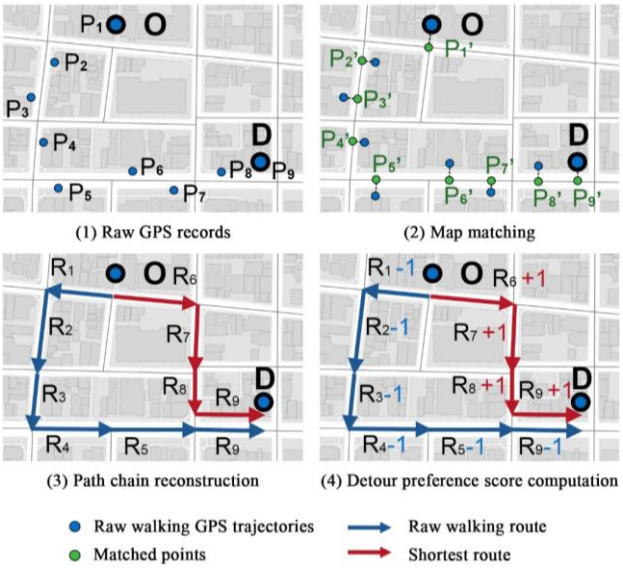


Figure 3. pedestrian detour preference score computation

3.3.1 Data Source

In this study, a large GPS dataset named "Torima" was utilized. "Torima" is an individual-level GPS location dataset provided by Geo Technologies Co., Ltd. It was collected through the "Torima" APP from phones with the AUTO-GPS function enabled. APP users have consented to the terms and conditions of the service for recording and analyzing their trajectories. Before being released to the authors, this dataset underwent preprocessing by GeoTechnologies, Inc. The preprocessing ensured that no linkage could be made between the data and any individual user. The dataset does not include specific personal information such as names, ages, or genders. The privacy of the data complies with Japanese law. This dataset contains approximately 1 billion GPS records collected from March 1, 2022, to March 31, 2022, spanning the entirety of Japan. The raw GPS location data (latitude, longitude, and timestamps) are sent approximately every 1 minute. GPS trajectories come with mobility mode labels, including: still, walking, running, vehicle, bicycle. We extracted records with mobility mode labeled as "walking."

3.3.2 Map Matching

Due to the urban canyon effect and inherent precision issues, GPS location records obtained from mobile phone often deviate from the actual road segments (**Figure3(a)**). To address this issue, we need to match the GPS points to the road segments (**Figure 3(b)**). Firstly, we downloaded the road segement shapefile from Open Street Map (OSM). All polyline were broken down into individual lines. The study area comprises 7624 road line segments in total, with unique IDs ranging from 1 to 7624. Then, map matching algorithm was used to find the matching

points of the GPS trajectory points on the road segments. The principle of this algorithm involves drawing perpendicular lines from the GPS points to nearby road segments, and the point on the line with the shortest perpendicular distance is chosen as the matching point, as it represents the most likely position of the GPS on the road segment. If $X_{(raw,u)} = \{P_1, P_2, P_3, \dots, P_t\}$ denotes a set of walking GPS locations of user u where P_t is the location at time stamp t,

$$P_t' = argmin\left(verticaldis(P_t, R_j)\right) \quad (1)$$
$$R_j \in \mathrm{R},$$
$$\mathrm{j} \in (1,7624)$$

In equation (1),P_t represents the original walking GPS record point, P_t' is the point matched onto the road segment, R_j denotes the road segment with ID j, and $verticaldis$ is a function that calculates the perpendicular distance between the original GPS point and the road segment.

3.3.3 Path Chain Reconstruction

To compute the pedestrian walking routes, it's essential to reconstruct the segment chain for each route. Firstly, we applied Topological algorithm to all road segments. The network of road segments can be represented as a graph, G. Each road segment constitutes an edge of the graph. The endpoints of the road segments are the graph's nodes, with each endpoint assigned a unique ID based on the logical connection of the road segmentation. We then employed the Dijkstra algorithm to determine the shortest path between two matched GPS points. The Dijkstra algorithm returns a set of road segment through which the user has traveled. This process is carried out in the pgRouting module of PostgreSQL.

For each walking trajectory record X_u of user u, the starting point of the trajectory is defined as P_O, and the endpoint is defined as P_O. We applied the path chain reconstruction method to $X_{(OD,u)} = \{P_O, P_D\}$ and it will returns a set of road segment $R_{(OD,u)}$ which refers to the shortest route between P_O and P_D . We also applied the path chain reconstruction method to $X_{(raw,u)} = \{P_1, P_2, P_3, \dots, P_t\}$ and it will returns a set of road segment numbers $R_{(raw,u)}$ through which the user has actually traveled (**Figure 3(c)**).

3.3.4 Computation of of Detour Preference Score

We use R_j to represent the road segment with ID j, $S(R_j)$ refers to the detour preference score of R_j. For each R_j in $R_{(raw,u)}$, the detour preference score will add 1; For each R_j in $R_{(OD,u)}$, the detour preference score will minus 1. **Figure 3(d)** is the example of the computation process. The higher the positive score, the more a path is chosen by pedestrians. The higher the negative score, the less a path is chosen. A score of 0 for a segment indicates no pedestrian preference.

Following is the pseudocode of detour preference score computation:

$R_j \in \mathrm{R}$

$\mathrm{j} \in (1,32649)$

for R_j in R:

  $S(R_j) = 0$

  for u in users:

    for R_j in $R_{(raw,u)}$:

      $S(R_j) \mathrel{+}= 1$

    for R_j in $R_{(OD,u)}$:

      $S(R_j) \mathrel{+}= -1$

3.4 Independent Variables: Built Environment Attributes

This section introduces the independent variables we used in this research.

3.4.1 Eye-level Street Environment Features

The eye-level street environment features are caculated using Google SVIs, CV and deep learning.

Downloading Google SVIs: SVI provides an eye-level view of the street environment that is close to the perception of pedestrians. Previous research [17], [18] have illustrated how a SVI sampled from street centerline could be useful to proxy pedestrians' view. SVI audit is also reliable given its inter- and intra-rater consistency and its high agreement with in-person street audits [19], [20]. In this research, All SVIs we use are obtained through the Google Street View Image Application Programming Interface (API). Google SVIs are taken by street view cars along streets that snap panoramas at around 1.5m high.

We sampled SVIs every 25 m along the public street's centerlines. The sampling process is conducted in QGIS, and the geographic coordinates of sampling points are obtained. By giving Google Street View API unique coordinates, each sampling point's SVI could be downloaded. To best proxy the pedestrian view walking along the street, we keep the same camera settings (heading: parallel with the street, the horizontal field of view: 120 degrees, the pitch angle of the camera: 0 degree) and image reso-

lution (640 pixels x 480 pixels) to get consistent sampling results. In total, we download 12051 valid SVIs.

Semantic Segmentation: We conduct image segmentation using the Pyramid Scene Parsing Network (PspNet) [21] under the open source deep learning framework in the GluonCV. PspNet has been widely used in urban studies [22]–[24] and has achieved high accuracy on the several streetscape datasets [25]–[28]. We use the psp_resnet101_ade pre-trained model (Apache MXNet, n.d.; PspNet Pre-Trained Model, n.d.; Segmentation — Gluoncv 0.11.0 Documentation, n.d.). With PSPNet, we can classify and distinguish different visual elements from each other in the SVIs.

View Indices Computation: We computed the view indices for each image, which represent the proportion of pixels occupied by a specific visual element in an SVI [29]. Examples of typical view indices include tree, building, and road, which describe the percentage of pixels occupied by these features in an image. We calculated the index of each visual feature in the SVIs using the following approach:

$$VI_{fea} = \sum_{i=1}^{n} PIXEL_{fea} \; / \; \sum_{i=1}^{n} PIXEL_{total} \quad (3)$$

Finally, 27 view indices are calculated includes: building, sky, sidewalk, tree, fence, plant, grass, wall, windowpane, fountain, water, signboard, railing, chair, road, streetlight, sculpture, awning, bridge, booth, ashcan, ceiling, mountain, column, lamp, earth, bulletin.

3.4.2 Other Independent Variables

We also take transportation, POIs, Nature condiction, and road level condiction into the model. These variables are thought to have impacts on walking behavior in existing studies. We obtained information on these features from Open Street Map (OSM) and National Land Information Platform.

For transportation condition, we compute the network distance of each road segment to the nearest metro station. And we also Number of bus stop within 250m buffer.

For POI, we compute the number of number of restaurant and shop within 250 m beffer of the road segment.

For nature condition, we computer the network distance of the road segment to the nearest park and river.

For road level, we use dummy variable to present the road category: trunk, primary, secondary, tertiary, residential, other roads.

3.5 Correlation Analysis

We aggregate all the information above into the road segement. The preference score of each road segment is the dependent variable in this research. First, Pearson correlation analysis is conducted between the preference score and the chosen variables. Only those variables indicating statistically significant correlations with preferences score were selected for regression analysis. The variables unrelated to the preference score are removed. Second, we analyzed each group of attributes using OLS (Ordinary Least Squares) model separately to scrutinize their explanatory power. The analytical processes mentioned above were conducted in Statsmodels Library in Python.

The model can be written as follows:

$$S(R_j) = \beta_0 + \sum_k \beta_k X_{jk} + \varepsilon_j$$

where $S(R_j)$ is walking preference score at observation road j; X_{jk} is independent variable k at observation j; β_k are the coefficient of independent variable k. ε_j an error term at observation j. β_0 are the intercept.

4. RESULTS

4.1 Descriptive Results

Table 1 gives the descriptive statistics of all variables used in this study.

Due to a large number of variables, not all of them can be detailed. We only selected some of variables indicating statistically significant correlations with preference score to shows the spatial distributions (**Figure 4**).

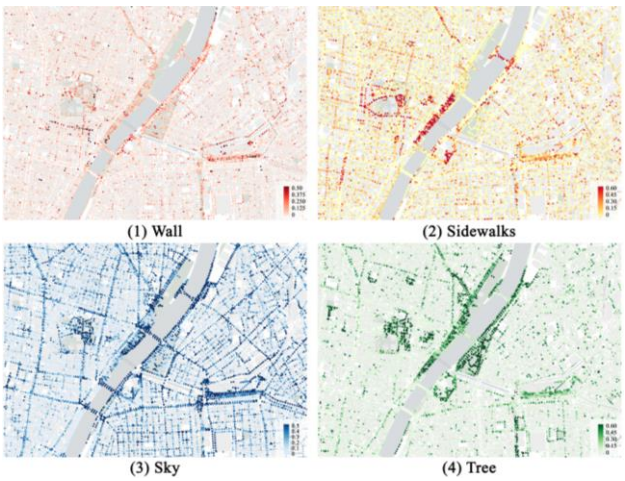


Figure 4. Example of the street view indiexs

Table 1. Description of the variables

	Definition	Mean	Std	Min	25%	50%	75%	Max
Independent Variables								
Preference Score	Preference Score of road segments	23.584470	52.466134	-114	3.000000	10.000000	25.000000	877
Dependent Variables								
SVI View Indices								
SVI_building	SVI visual ratio	0.403206	0.180347	0.000000	0.287319	0.430206	0.534863	0.995555
SVI_sky	SVI visual ratio	0.116566	0.077959	0.000000	0.064566	0.095835	0.149750	0.472238
SVI_sidewalk	SVI visual ratio	0.055907	0.072667	0.000000	0.012993	0.029264	0.065594	0.434785
SVI_tree	SVI visual ratio	0.064641	0.098136	0.000000	0.001015	0.018202	0.086947	0.615672
SVI_fence	SVI visual ratio	0.011515	0.027286	0.000000	0.000000	0.001093	0.009899	0.366988
SVI_plant	SVI visual ratio	0.021914	0.035456	0.000000	0.001184	0.008303	0.026902	0.358371
SVI_grass	SVI visual ratio	0.005155	0.020676	0.000000	0.000000	0.000000	0.000544	0.445781
SVI_wall	SVI visual ratio	0.019898	0.048426	0.000000	0.000000	0.001208	0.015838	0.481105
SVI_windowpane	SVI visual ratio	0.000225	0.002685	0.000000	0.000000	0.000000	0.000000	0.102703
SVI_fountain	SVI visual ratio	0.000021	0.000632	0.000000	0.000000	0.000000	0.000000	0.032105
SVI_water	SVI visual ratio	0.004092	0.033224	0.000000	0.000000	0.000000	0.000000	0.493348
SVI_signboard	SVI visual ratio	0.003038	0.006663	0.000000	0.000000	0.000609	0.003354	0.183215
SVI_railing	SVI visual ratio	0.004120	0.015980	0.000000	0.000000	0.000000	0.000035	0.242461
SVI_chair	SVI visual ratio	0.000066	0.000739	0.000000	0.000000	0.000000	0.000000	0.027000
SVI_road	SVI visual ratio	0.228510	0.125052	0.000000	0.140580	0.253922	0.328234	0.462363
SVI_streetligh	SVI visual ratio	0.000372	0.000975	0.000000	0.000000	0.000006	0.000298	0.014980
SVI_sculpture	SVI visual ratio	0.000027	0.000613	0.000000	0.000000	0.000000	0.000000	0.030199
SVI_awning	SVI visual ratio	0.000838	0.004841	0.000000	0.000000	0.000000	0.000000	0.128863
SVI_bridge	SVI visual ratio	0.001281	0.008305	0.000000	0.000000	0.000000	0.000000	0.180168
SVI_booth	SVI visual ratio	0.000028	0.000982	0.000000	0.000000	0.000000	0.000000	0.063836
SVI_ashcan	SVI visual ratio	0.000171	0.000941	0.000000	0.000000	0.000000	0.000000	0.022695
SVI_ceiling	SVI visual ratio	0.003487	0.026854	0.000000	0.000000	0.000000	0.000000	0.487738
SVI_mountain	SVI visual ratio	0.000104	0.002720	0.000000	0.000000	0.000000	0.000000	0.156543
SVI_column	SVI visual ratio	0.000535	0.006633	0.000000	0.000000	0.000000	0.000000	0.272430
SVI_lamp	SVI visual ratio	0.000002	0.000061	0.000000	0.000000	0.000000	0.000000	0.004383
SVI_earth	SVI visual ratio	0.010504	0.038871	0.000000	0.000000	0.000000	0.001288	0.425992
SVI_bulletin	SVI visual ratio	0.000104	0.001683	0.000000	0.000000	0.000000	0.000000	0.061789
Transportation								
Metro_Dis	Network distance to the nearest metro station	525.651659	303.570802	0.000000	288.476043	469.534038	724.273561	1499.839473
BusStop	Number of bus stop within 250m buffer	2.254402	2.563824	0.000000	0.000000	1.000000	4.000000	13.000000
POI								
Restaurant	Number of restaurant within 250m buffer	5.743791	11.636816	0.000000	0.000000	2.000000	5.000000	74.000000
Shop	Number of shop within 250m buffer	1.349222	2.481840	0.000000	0.000000	0.000000	2.000000	19.000000
Nature condition								
Park_Dis	Distance to the nearest park	219.882824	136.574892	0.270964	110.277929	215.850561	324.466757	564.446160
River_Dis	Distance to the river	599.509384	382.223684	10.130197	260.639353	561.804057	887.362082	1623.596697
Road Level								
Trunk	Dummy variable, 1:Yes/0:No	-	-	0	-	-	-	1
Primary	Dummy variable, 1:Yes/0:No	-	-	0	-	-	-	1
Secondary	Dummy variable, 1:Yes/0:No	-	-	0	-	-	-	1
Tertiary	Dummy variable, 1:Yes/0:No	-	-	0	-	-	-	1
Residential	Dummy variable, 1:Yes/0:No	-	-	0	-	-	-	1
Other_road	Dummy variable, 1:Yes/0:No	-	-	0	-	-	-	1

4.2 Preferences Score Computation Results

Figure 5 shows the preference score of the study area. The road of Tokyo skytree surrounding area, path along Sumida Park, Tobu Sumida River Walk, connection path between Kaminarimon and Sensoji Temple show high positive preferences score. People are willing to take long detours route to choose these roads for walking.

Fuji Road, Fureai Road, Kukojima Road and Kaminarimonnaka Roan shows high negative preferences score. People are not willing to choose these roads for walking although these road may be shorter.

4.3 Effects of the Attributes

Although **Figure 5** shows the distribution trend of

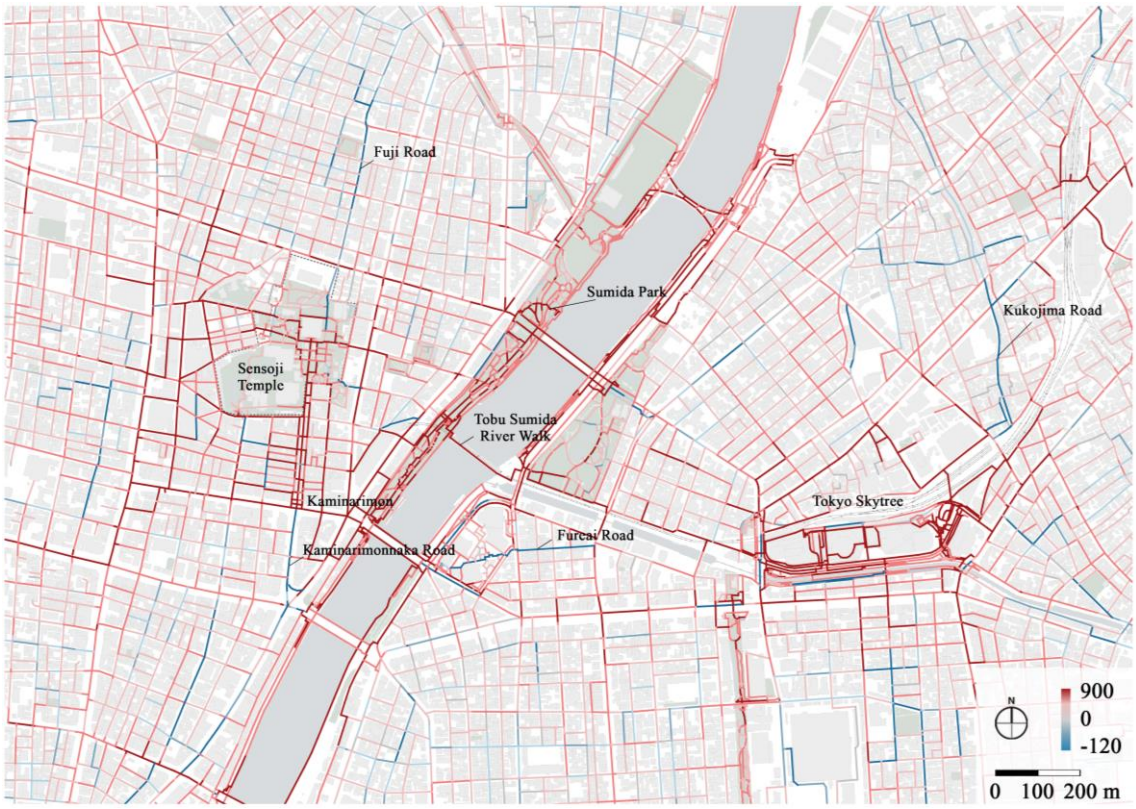


Figure 5. Preference score of the study area

pedestrian preference streets, we need to use model to more accurately quantify the impact of environmental factors. We first conduct Variance Inflation Factor (VIF) test to examine the collinearity of the dependent variables. The variable with VIF larger than 10 (building) are removed. OLS is conducted for the remained variables. The R square of the model is 0.522, which is acceptable.

Table 2 shows the OLS regression result. For SVI view indices, the visual ratio of sky, sidewalk, tree, grass, wall, water, road, streetlight, bridge, booth, ceiling, column shows significant impact on 0.05 significance level.

Among those variables, sky, sidewalk, tree, grass, water, railing , road, streetlight, bridge, booth, ceiling, column show positive impact. Trees and grass are revealed as positive influencing variables. Street greening provides aesthetic and ecological value to the community, and thus is considered an indicator of positive walking behavior in the built environment. The positive impact of street lights on walking can likely be explained by safety concerns. In the presence of streetlights, they might offer sufficient traffic perceptual safety, serving as a driving factor in route choice. Both roads and sidewalks have positively implied route selection, which is supported by prior research. An increase in road pixels might lead to wider roads, which are more likely to have walkways. Ceilings provide shade for pedestrian walking, which might serve as a driving force in route selection. Wall and railing shows negative impact. People might not like the enclosed feeling brought by walls and railings.

For transportation, the distance to the nearest metro station shows significant negative impact. More close to the metro station, the higher the preferences score is. The number of bus stop shows significant positive impact. The more the bus station are, the higher the preferences score is. There are several possible reason. First, better public transportation facilities can promote walking. Secondly, for those people who have to rely on public transport to travel, they have to make detours to reach public stops.

For POI, number of restaurants and shop has significant positive impact on preference socre. The Thriving commerce can encourage people to walk.

For nature condition, distance to park and river all have significant negative impacts on preference score. More close to the park and river, the higher the preferences score is. People are willing to wandering in places with beautiful natural surroundings.

For road level, only residential road has significant impact on preference. People are not willing to walk in residential level road. This can likely be explained by safety concerns. The residential level road might not provide enough perceptual safety for walking.

Table 2 . OLS model

R-squared: 0.522

Attributes	Coef.	Std.Err.	t	P>|t|	[0.025	0.975]
const	31.314	9.598	3.263	***	12.499	50.129
SVI View Indices						
SVI_sky	93.155	8.690	10.719	***	76.120	110.191
SVI_sidewalk	36.564	10.858	3.368	***	15.280	57.848
SVI_tree	10.822	7.742	1.398	***	4.354	25.998
SVI_fence	-26.920	21.340	-1.261		-68.753	14.913
SVI_plant	14.028	17.408	0.806		-20.096	48.153
SVI_grass	81.784	30.084	2.719	***	22.812	140.757
SVI_wall	-58.433	13.638	-4.285	***	-85.167	-31.699
SVI_windowpane	-63.951	200.843	-0.318		-457.659	329.757
SVI_fountain	-19.738	842.029	-0.023		-1670.349	1630.872
SVI_water	48.142	18.153	2.652	***	12.558	83.726
SVI_signboard	26.804	82.804	0.324		-135.514	189.123
SVI_railing	-151.992	38.158	-3.983	***	-226.792	-77.191
SVI_chair	-1836.026	720.285	-2.549		-3247.984	-424.067
SVI_road	28.907	8.119	3.560	***	12.992	44.822
SVI_streetlight	2265.273	567.615	3.991	***	1152.591	3377.955
SVI_sculpture	-1593.002	886.410	-1.797		-3330.611	144.607
SVI_awning	-158.247	111.606	-1.418		-377.024	60.531
SVI_bridge	199.499	66.576	2.997	***	68.992	330.005
SVI_booth	1875.280	545.353	3.439	***	806.238	2944.323
SVI_ashcan	-858.603	571.506	-1.502		-1978.912	261.706
SVI_ceiling	415.583	23.465	17.711	***	369.585	461.580
SVI_mountain	-133.471	197.810	-0.675		-521.234	254.292
SVI_column	412.474	86.320	4.778	***	243.263	581.685
SVI_lamp	619.138	8733.112	0.071		-16500.000	17700.000
SVI_earth	16.495	17.484	0.943		-17.779	50.770
SVI_bulletin	-349.974	316.546	-1.106		-970.491	270.543
Transportation						
Metro_Dis	-0.027	0.002	-12.451	***	-0.031	-0.023
BusStop	4.385	0.280	15.655	***	3.836	4.934
POI						
Restaurant	0.694	0.091	7.651	***	0.516	0.871
Shop	3.407	0.420	8.105	***	2.583	4.231
Nature condition						
Park_Dis	-0.032	0.004	-7.208	***	-0.041	-0.023
River_Dis	-0.002	0.002	-0.964	***	-0.005	0.002
Road Level						
Trunk	-20.177	10.274	-1.964		-40.318	-0.036
Primary	-17.802	9.989	-1.782		-37.384	1.780
Secondary	-17.125	9.454	-1.811		-35.658	1.408
Tertiary	-14.833	9.218	-1.609		-32.903	3.237
Residential	-22.633	9.033	-2.506	**	-40.341	-4.926
Other_road	-8.626	9.072	-0.951		-26.410	9.157

p values are shown in parentheses; *** and ** indicate a significance level of 0.01 and 0.05, respectively.

5. CONCLUSION

This study utilizes large-scale individual-level GPS trajectories and proposes a novel score that reflects the pedestrian detour preference for each street. By integrating SVI data with CV techniques, we measured micro-scale built environment features and quantified the influence of micro-level built envi-ronment factors on individual detour behaviors.

The results show the effectiveness of our proposed preference score in describing the pedestrians' walking preferences and rout choice. We identify the roads that people actively choose and negatively choose. We also reveal the influence of micro-level built envi-ronment factors on individual detour behaviors. The street element such as sidewalk, tree, grass, wall, water, road, streetlight, ceiling can promote walking choice, transportation, POI and nature condition also promote walking choice. The result will provide insights for urban planners and policymakers to craft a supportive walking environment to

sustainably increase walking activities This study offers valuable insights for designing guidelines and interventions promoting sustainable lifestyles.

ACKNOWLEDGMENTS

The authors would like to thank GeoTechnologies, Inc. (ジオテクノロジーズ株式会社) and LocationMind Inc (LocationMind株式会社) for providing walking trip data. This research could not have been made without the data support from GeoTechnologies, Inc. and LocationMind Inc.

APPENDIX

Appendix 1. VIF Test result

Feature	VIF
SVI_sky	1.634802
SVI_sidewalk_mean	2.21719
SVI_tree	2.055908
SVI_fence	1.207658
SVI_plant	1.356838
SVI_grass	1.378021
SVI_wall	1.553505
SVI_windowpane	1.035893
SVI_fountain	1.008253
SVI_water	1.295482
SVI_signboard	1.084265
SVI_railing	1.324352
SVI_chair	1.008217
SVI_road	3.671351
SVI_streetligh	1.090334
SVI_sculpture	1.053052
SVI_awning	1.039672
SVI_bridge	1.088904
SVI_booth	1.021167
SVI_ashcan	1.029388
SVI_ceiling	1.414115
SVI_mountain	1.030947
SVI_column	1.167614
SVI_lamp	1.010285
SVI_earth	1.645128
SVI_bulletin	1.010791
Metro_Dis	1.547054
BusStop	1.836723
Restaurant	3.964511
Shop	3.876967
Park_Dis	1.310801
River_Dis	1.459264
Trunk	-
Primary	-
Secondary	-
Tertiary	-
Residential	-
Other_road	-

Appendix 2.

Dijkstra's algorithm is a widely used approach to finding the shortest path between any two vertices of a graph [30], [31]. $P = \{P_1, P_2, P_3, \dots, P_{t-1}, P_t, \dots\}$ denotes a set of raw GPS points of one route. After applying map matching and topology algorithm described in section3.3.1, the road network can be represented as a graph structure G. Each road segmentation is an edge of the graph. Each intersection point of the road segmentations is a node of the graph and is given a unique ID according to the logical connection of road segmentations. Q denotes the set of all nodes in G.

R'_{t-1} denotes the road segmentation on which P_{t-1} matched. R'_t denotes the road segmentation on which P_t matched. $Source$ refers to the start vertex of R'_{t-1} and $Target$ refers to the start vertex of R'_{t-1}. The followings are the pseudo code for Dijkstra algorithm:

```
function Dijkstra(Graph, Source, Target):
        for each vertex v in Graph:
          dist [v] ← infinity
          prev[v] ← undefined
          add v to Q
        dist[Source] ← 0
        while Q is not not empty:
          u ← vertex in Q with min dist[u]
          remove u from Q

                S ← empty sequence
                u ← Target
                if prev[u] is defined or u = Source:
                        while u is defined:
                                insert u at the beginning of S
                                u ← prev[u]
                for each neighbor v of u still in Q:
                        alt ← dist[u] + dist_between (u, v)
                        if  alt < dist[v]:
                        dist[v] ← alt
                        prev[v] ← u

        return prev[ ], dist[ ]
```

By this way, we obtain a set of the road segmentation ID between R'_{t-1} and R'_{t-1}. We iterate this searching process for $P = \{P_1, P_2, P_3, \dots, P_{t-1}, P_t, \dots\}$ and finally reconstruct the chain of road segments for each route.

REFERENCES

[1]S. L. Handy, M. G. Boarnet, R. Ewing, and R. E. Killingsworth, "How the built environment affects

physical activity: Views from urban planning," American Journal of Preventive Medicine, vol. 23, no. 2, Supplement 1, pp. 64–73, Aug. 2002, doi: 10.1016/S0749-3797(02)00475-0.
[2] B. E. Saelens and S. L. Handy, "Built environment correlates of walking: a review," Medicine and science in sports and exercise, vol. 40, no. 7 Suppl, p. S550, 2008.
[3] M. Kamruzzaman, S. Washington, D. Baker, W. Brown, B. Giles-Corti, and G. Turrell, "Built environment impacts on walking for transport in Brisbane, Australia," Transportation, vol. 43, pp. 53–77, 2016.
[4] R. Cervero, O. L. Sarmiento, E. Jacoby, L. F. Gomez, and A. Neiman, "Influences of Built Environments on Walking and Cycling: Lessons from Bogotá," International Journal of Sustainable Transportation, vol. 3, no. 4, pp. 203–226, Jun. 2009, doi: 10.1080/15568310802178314.
[5] T. Feuillet et al., "Built environment in local relation with walking: Why here and not there?," Journal of Transport & Health, vol. 3, no. 4, pp. 500–512, 2016.
[6] C. E. T. Neves, A. R. Da Silva, and F. S. de Arruda, "Exploring the link between built environment and walking choice in São Paulo city, Brazil," Journal of transport geography, vol. 93, p. 103064, 2021.
[7] A. V. Moudon and C. Lee, "Walking and Bicycling: An Evaluation of Environmental Audit Instruments," Am J Health Promot, vol. 18, no. 1, pp. 21–37, Sep. 2003, doi: 10.4278/0890-1171-18.1.21.
[8] A. M. Larrañaga, L. I. Rizzi, J. Arellana, O. Strambi, and H. B. B. Cybis, "The influence of built environment and travel attitudes on walking: A case study of Porto Alegre, Brazil," International Journal of Sustainable Transportation, vol. 10, no. 4, pp. 332–342, Apr. 2016, doi: 10.1080/15568318.2014.933986.
[9] S. Kim, S. Park, and K. Jang, "Spatially-varying effects of built environment determinants on walking," Transportation research part A: policy and practice, vol. 123, pp. 188–199, 2019.
[10] B. Kang, A. V. Moudon, P. M. Hurvitz, and B. E. Saelens, "Differences in behavior, time, location, and built environment between objectively measured utilitarian and recreational walking," Transportation research part D: transport and environment, vol. 57, pp. 185–194, 2017.
[11] A. Salazar Miranda, Z. Fan, F. Duarte, and C. Ratti, "Desirable streets: Using deviations in pedestrian trajectories to measure the value of the built environment," Computers, Environment and Urban Systems, vol. 86, p. 101563, Mar. 2021, doi: 10.1016/j.compenvurbsys.2020.101563.
[12] C. Bongiorno et al., "Vector-based pedestrian navigation in cities," Nature Computational Science, vol. 1, no. 10, pp. 678–685, 2021.
[13] G. Gao, Z. Wang, X. Liu, Q. Li, W. Wang, and J. Zhang, "Travel behavior analysis using 2016 Qingdao's household traffic surveys and Baidu electric map API data," Journal of Advanced Transportation, vol. 2019, 2019, Accessed: Oct. 13, 2023. [Online]. Available: https://www.hindawi.com/journals/jat/2019/6383097/abs/
[14] Z. Zheng, W. Shen, Y. Li, Y. Qin, and L. Wang, "Spatial equity of park green space using KD2SFCA and web map API: A case study of zhengzhou, China," Applied Geography, vol. 123, p. 102310, 2020.
[15] K. Duchowny, P. Clarke, N. A. Gallagher, R. Adams, A. L. Rosso, and N. B. Alexander, "Using Mobile, Wearable, Technology to Understand the Role of Built Environment Demand for Outdoor Mobility," Environment and Behavior, vol. 51, no. 6, pp. 671–688, Jun. 2019, doi: 10.1177/0013916517749256.
[16] Y. Hahm, H. Yoon, and Y. Choi, "The effect of built environments on the walking and shopping behaviors of pedestrians; A study with GPS experiment in Sinchon retail district in Seoul, South Korea," Cities, vol. 89, pp. 1–13, 2019.
[17] K. Ito and F. Biljecki, "Assessing bikeability with street view imagery and computer vision," Transportation research part C: emerging technologies, vol. 132, p. 103371, 2021.
[18] X. Ma et al., "Measuring human perceptions of streetscapes to better inform urban renewal: A perspective of scene semantic parsing," Cities, vol. 110, p. 103086, 2021.
[19] L. He, A. Páez, and D. Liu, "Built environment and violent crime: An environmental audit approach using Google Street View," Computers, Environment and Urban Systems, vol. 66, pp. 83–95, 2017.
[20] A. G. Rundle, M. D. Bader, C. A. Richards, K. M. Neckerman, and J. O. Teitler, "Using Google Street View to audit neighborhood environments," American journal of preventive medicine, vol. 40, no. 1, pp. 94–100, 2011.
[21] H. Zhao, J. Shi, X. Qi, X. Wang, and J. Jia, "Pyramid scene parsing network," in Proceedings of the IEEE conference on computer vision and pattern recognition, 2017, pp. 2881–2890.
[22] L. Chen et al., "Measuring impacts of urban environmental elements on housing prices based on multisource data—a case study of Shanghai, China," ISPRS International Journal of Geo-Information, vol. 9, no. 2, p. 106, 2020.
[23] X. Fu, T. Jia, X. Zhang, S. Li, and Y. Zhang, "Do street-level scene perceptions affect housing prices in Chinese megacities? An analysis using open access datasets and deep learning," PloS one, vol. 14, no. 5, p. e0217505, 2019.

[24] N. Su, W. Li, and W. Qiu, “Measuring the associations between eye-level urban design quality and on-street crime density around New York subway entrances,” Habitat International, vol. 131, p. 102728, 2023.
[25] C.-Y. Lin, Y.-C. Chiu, H.-F. Ng, T. K. Shih, and K.-H. Lin, “Global-and-local context network for semantic segmentation of street view images,” Sensors, vol. 20, no. 10, p. 2907, 2020.
[26] H. Ning, X. Ye, Z. Chen, T. Liu, and T. Cao, “Sidewalk extraction using aerial and street view images,” Environment and Planning B: Urban Analytics and City Science, vol. 49, no. 1, pp. 7–22, 2022.
[27] Y. Xia, N. Yabuki, and T. Fukuda, “Development of a system for assessing the quality of urban street-level greenery using street view images and deep learning,” Urban Forestry & Urban Greening, vol. 59, p. 126995, 2021.
[28] H. Zhou et al., “Using Google Street View imagery to capture micro built environment characteristics in drug places, compared with street robbery,” Computers, Environment and Urban Systems, vol. 88, p. 101631, 2021.
[29] X. Li, Y. Zhang, L. Sun, and Q. Liu, “Free-floating bike sharing in jiangsu: Users’ behaviors and influencing factors,” Energies, vol. 11, no. 7, p. 1664, 2018.
[30] D. B. Johnson, “A Note on Dijkstra’s Shortest Path Algorithm,” J. ACM, vol. 20, no. 3, pp. 385–388, Jul. 1973, doi: 10.1145/321765.321768.
[31] F. Schulz, D. Wagner, and K. Weihe, “Dijkstra’s algorithm on-line: an empirical case study from public railroad transport,” ACM J. Exp. Algorithmics, vol. 5, pp. 12-es, Dec. 2001, doi: 10.1145/351827.384254.